Nano Research 2018, 11(5): 2592–2604
https://doi.org/10.1007/s12274-017-1885-8
Research Article
ISSN 1998-0124
CN 11-5974/O4

Programmable DNA-responsive microchip for the capture and release of circulating tumor cells by nucleic acid hybridization

Shan Guo[1,§], Haiyan Huang[1,§], Xujing Deng[2], Yuqi Chen[1], Zhuoran Jiang[1], Min Xie[3], Songmei Liu[2], Weihua Huang[3] (✉), and Xiang Zhou[1] (✉)

[1] *College of Chemistry and Molecular Sciences, the Institute for Advanced Studies of Wuhan University, Hubei Province Key Laboratory of Allergy and Immunology, Wuhan University, Wuhan 430072, China*
[2] *Zhongnan Hospital, Wuhan University, Wuhan 430072, China*
[3] *Key Laboratory of Analytical Chemistry for Biology and Medicine (Ministry of Education), College of Chemistry and Molecular Sciences, Wuhan University, Wuhan 430072, China*
[§] *Shan Guo and Haiyan Huang contributed equally to this work.*

Received: 16 March 2017
Revised: 11 October 2017
Accepted: 13 October 2017

KEYWORDS

DNA-responsive microchip,
hierarchical architecture,
circulating tumor cells (CTCs),
aptamer,
capture,
release,
nucleic acid hybridization

ABSTRACT

The detection and analysis of circulating tumor cells (CTCs) from patients′ blood is important to assess tumor status; however, it remains a challenge. In the present study, we developed a programmable DNA-responsive microchip for the highly efficient capture and nondestructive release of CTCs via nucleic acid hybridization. Transparent and patternable substrates with hierarchical architectures were integrated into the microchip with herringbone grooves, resulting in greatly enhanced cell-surface interaction via herringbone micromixers, more binding sites, and better matched topographical interactions. In combination with a high-affinity aptamer, target cancer cells were specifically and efficiently captured on the chip. Captured cancer cells were gently released from the chip under physiological conditions using toehold-mediated strand displacement, without any destructive factors for cells or substrates. More importantly, aptamer-containing DNA sequences on the surface of the retrieved cancer cells could be further amplified by polymerase chain reaction (PCR), facilitating the detection of cell surface biomarkers and characterization of the CTCs. Furthermore, this system was extensively applied to the capture and release of CTCs from patients′ blood samples, demonstrating a promising high-performance platform for CTC enrichment, release, and characterization.

Address correspondence to Xiang Zhou, xzhou@whu.edu.cn; Weihua Huang, whhuang@whu.edu.cn

1 Introduction

Circulating tumor cells (CTCs), propagating from either primary or metastatic tumors, have evoked considerable interest within the fields of cancer diagnosis and therapy. Studies have proposed that CTCs could be used as valuable prognostic biomarkers, to evaluate the response to treatment, and could offer more powerful information to understand tumor metastasis [1]. However, detection of CTCs remains a tremendous technical challenge, because CTCs are extraordinarily rare events (a few to hundreds of CTCs per 10^9 cells of hematologic cells) and are heterogeneous.

Accordingly, significant research effort has been devoted to exploring a variety of techniques to isolate CTCs from blood, including gradient centrifugation [2, 3], size-based isolation [4–6], and affinity-based separation [7–27]. Among these methods, microfluidic devices integrated with micro/nanostructured substrates, as well as high affinity ligands, including antibodies and aptamers, have provided opportunities to improve the yield, sensitivity, and purity [14–18]. These integrated microchips benefitting from a high surface-area-to-volume ratio, increased capture agent presentation, and the scale of the extracellular structures can increase the interaction between the cells and the surface of the microchannels. Recent studies showed that compared with single vertical nanostructures (such as nanopillars [10]) and single horizontal nanostructures (such as nanofibers [11]), substrates with hierarchical architectures [28–31] exhibited significantly enhanced cell-capture performance. Thus, a hierarchical nanostructure-integrated microfluidic device should be a promising platform for CTC isolation. Additionally, in contrast to antibody ligands, cell-systematic evolution of ligands by exponential enrichment (SELEX) aptamers possess significant advantages, such as long-term stability, synthetic reproducibility, and easy chemical modification [32]. However, aptamer-based methods have rarely been used for CTC isolation from patients′ blood samples.

Beyond the efficient capture and enumeration of CTCs, it is critical to gently release CTCs from devices for in-depth characterization and to study the properties of these cells. To address this issue, methods based on photosensitive-induced cleavage [5, 33, 34], electrochemical desorption [28, 35], thermodynamic release [36–38], chemical reagent-triggered substrate sacrifice [31, 39], and competition-based ligand replacement [32, 40], have been developed to detach cells from antibody-coated surfaces. However, many of these strategies have limitations, such as dangerous ultraviolet light, cytotoxic chemical molecules, and strict processing conditions. For aptamers as capturing agents for cell-capture systems, enzymes are mainly used to effectively release the cells [16], which is potentially destructive to cells. Therefore, devices with high-performance capture and nondestructive release properties remain desirable for CTC assays.

In the present study, we developed a programmable DNA-responsive microchip for high-performance capture and release of CTCs via nucleic acid hybridization. The overall concept is illustrated in Scheme 1. Target cancer cells are homogeneously tagged by hybridized aptamers against epithelial cell adhesion molecule (EpCAM) (AB, sequence B prehybridized with biotinylated sequence A). Then, benefiting from the greatly enhanced cell-substrate interaction resulting from herringbone-induced micro-vortices and better-matched topographical interactions, cancer cells are specifically and efficiently captured on the chip by the high-affinity streptavidin-biotin interaction. To nondestructively release the cancer cells, sequence C is employed to trigger dissociation

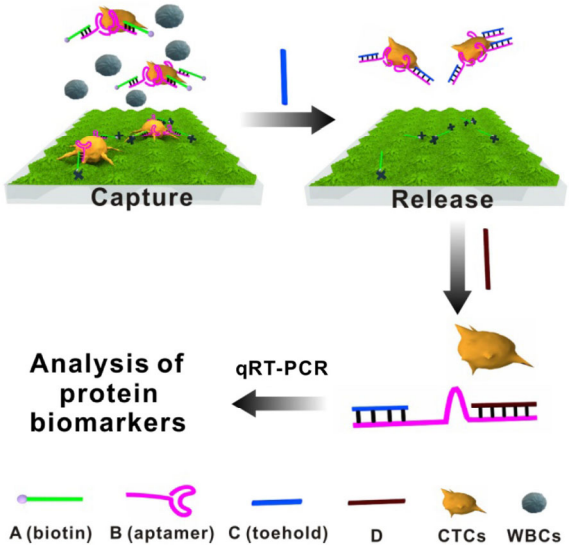

Scheme 1 Schematic illustration of programmable DNA-responsive microchip integrated with hierarchical substrates for the capture, release, and detection of protein biomarkers of CTCs.

of sequence B from hybridized aptamer A (toehold-mediated strand displacement, AB + C = A + BC), resulting in weakened cell-substrate interaction and effective cell release. More importantly, sequence B on the surface of retrieved cells could be released by sequence D_{48}, which is complementary to the anti-EpCAM aptamer, and further amplified by PCR, transforming the aptamer against the protein signature into a detectable and quantitative signal. These results make this programmable DNA-responsive microchip very promising for CTC detection and characterization.

2 Experimental

2.1 Materials

Zinc acetate dehydrate, zinc nitrate hexahydrate, and hexamethylenetetramine were obtained from Sinopharm Chemical Reagent Co., Ltd. (Shanghai, China). Carboxyethylsilanetriol Na salt, 25% in water, was purchased from J&K Scientific Co., Ltd. (Beijing, China). Phosphate-buffered saline (PBS) was prepared in the laboratory. 1-(3-Dimethylaminopropyl)-3-ethylcarbodiimide hydrochloride (EDC), Hoechst 33342, and streptavidin were purchased from Sigma-Aldrich. All oligonucleotides (Table S1 in the Electronic Supplementary Material (ESM)) were synthesized by Sangon Biotechnology Co., Ltd. (Shanghai, China). All media for cell culture were purchased from Gibco Corp. The non-enzymatic cell dissociation reagent was obtained from Qiyi Biological Technology Co., Ltd. (Shanghai, China). Calcein-acetoxymethyl (AM) and propidium iodide (PI) were purchased from Invitrogen. The UltraSYBR Mixture was obtained from CWbio. Co., Ltd. (Beijing, China). Blood samples were obtained from Zhongnan Hospital of Wuhan University. Fluorescein isothiocyanate (FITC)-labeled anti-cytokeratin 19 antibodies and PE-labeled anti-CD45 antibodies were purchased from Abcam Company. Alexa 488-conjugated antibodies against EpCAM were purchased from Cell Signaling Technology.

2.2 Characterization

Scanning electron microscopy (SEM) images were obtained using a field-emission scanning electron microscope (Zeiss SIGMA). Fluorescence microscopy (AxioObserver Z1, Zeiss, Germany) was used to image and identify cells. Quantitative real-time reverse transcription polymerase chain reaction (qRT-PCR) was performed using the Bio-Rad CFX96 system. Fluorescent signals from the polyacrylamide gels were detected using the Molecular Imager PharosFX™ System.

2.3 Preparation of the zinc-phosphate-based hierarchical nanostructure (HZnPNS)-embedded microfluidic chip

The HZnPNS-embedded microfluidic chip comprised a herringbone mixer device and a patterned HZnPNS. The mixer device was prepared using a standard soft lithography method. First, silicon wafers were spin-coated with 30-μm-thick SU-8 2015 photoresist as the main channel layer (length 12 cm and width 2.5 mm). Second, another layer (45-μm thick) of SU-8 2050 was added to form the herringbone mixer layer. These two steps produced a positive mold for the fabrication of the polydimethylsiloxane (PDMS) herringbone mixer. The PDMS prepolymer mixed with its crosslinker at a 10:1 weight ratio was poured on the mold, degassed, and allowed to cure in a conventional oven at 75 °C for 2 h. Finally, the cured PDMS replicas were peeled from the mold and two holes were punched at both ends of the fluidic channel to connect the tubing.

To obtain patterned HZnPNS, we first fabricated HZnPNS according to our previously reported method [31]. We then used photolithography and chemical wet etching to pattern this substrate. A thin film of photoresist (AZ 4620) was spin-coated onto the HZnPNS. After UV exposure and development, HZnPNS covered by the patterned photoresist was etched using diluted HCl. Finally, the patterned photoresist on the substrate was removed using acetone. After rinsing with deionized (DI) water and drying under nitrogen, the patterned HZnPNS was subjected to oxygen plasma treatment and bonded with the cured PDMS replicas to form the final device.

2.4 Modification of HZnPNS-embedded microfluidic chip with streptavidin

According to our previously reported method [31], 100 μL of PBS containing 20 μL of carboxyethylsilanetriol

solution was first flowed through the plasma-activated microfluidic chip at a flow rate of 10 μL·min^{-1}. After 3 h of incubation, the device was washed with DI water. Then, 25 mM EDC solution in boric acid buffer (10 mM, pH 7.4) was flowed through the device for 30 min at 20 μL·min^{-1} to activate the carboxylic groups. Subsequently, 40 μL (1 mg·mL^{-1}) of streptavidin was introduced to the device, followed by incubation for 4 h on ice.

To reduce non-specific adsorption, a solution of 5% (50 mg·mL^{-1}) bovine serum albumin (BSA), and 0.2% Tween-20 in PBS was used to inactivate the surface. Finally, FITC-labeled biotin (40 μL, 50 mg·mL^{-1}) was used to verify whether streptavidin was successfully conjugated onto the chip.

2.5 Gel electrophoresis

The aptamer-containing oligonucleotide sequence (B) and its primary complementary oligonucleotide (A) were mixed at a molar ratio of 1:1 to form a hybridized aptamer (AB) in PBS at 37 ℃ for 2 h. The secondary complementary oligonucleotide (C), at a final molar ratio of 2:1, was transferred to the solution and incubated at 37 ℃ for 0.5 h. The mixture was loaded into a 12% native polyacrylamide gel for electrophoresis (120 V, 60 min). All DNA sequences were labeled by carboxytetramethylrhodamine (TAMRA).

2.6 Fluorescent imaging of nucleic acid hybridization on the HZnPNS-embedded microfluidic chip

A solution (40 μL) of 1.25 μM hybridized aptamer (AB) was firstly flowed through the streptavidin-coated chip, followed by incubation for 30 min at room temperature. The chip was washed with PBS (10 μL·min^{-1}, 10 min) and imaged under an inverted fluorescence microscope. Sequence A was labeled by TAMRA and sequence B was labeled by FITC. To investigate the stability of the hybridized aptamer on the chip, the AB complex-modified chip was further incubated with PBS at 37 ℃ for 30 min and imaged. Then, 40 μL of 5 μM sequence C was flowed through the chip, followed by incubation at 37 ℃ for 30 min, washing, and imaging. Thereafter, the sequence A-coated chip was further incubated with 5 μM sequences B at 37 ℃ for 45 min, washed and imaged. The process of controlled association and dissociation with B was repeated three times in total. The fluorescent intensity was evaluated using the image processing software Image J.

2.7 Cell culture

MCF-7 cells (human breast cancer cell line) and HEK-293T cells (embryonic kidney cell line) were cultured in the high glucose (4.5 g·L^{-1}) version of Dulbecco's modified Eagle medium (DMEM), supplemented with 10% fetal bovine serum and 100 U·mL^{-1} penicillin-streptomycin. Both cells were maintained at 37 ℃ in a humidified incubator containing 5% CO_2. Cell detachment from the culture dishes was induced 5 mL of a non-enzymatic cell dissociation reagent at 37 ℃ for 10 min.

2.8 Cancer cell-capture assay

Before performing the cell-capture experiment, we investigated the specificity of the anti-EpCAM aptamer. EpCAM-positive MCF-7 cells, EpCAM-negative HEK-293T cells, and white blood cells (WBCs) (all 1 × 10^5 cells) were incubated with 500 nM TAMRA-labeled aptamers in culture medium on ice for 40 min. After being washed twice at 1,000 rpm for 8 min, the cells were resuspended in 1 × PBS for imaging. To obtain WBCs, healthy human blood samples were treated with red blood cell lysing buffer, according to the manufacturer's instructions. We then investigated whether the hybridized aptamer-tagged cells could be immobilized on the chip via the streptavidin-biotin interaction. Sequence A was modified with biotin and sequence B was labeled with TAMRA. Here, hybridized aptamer-tagged cancer cells were first incubated with streptavidin, and then FITC-labeled biotin was added to characterize that streptavidin was successfully labeled on the cell surface.

Subsequently, we optimized the flow rates for capturing target cancer cells. MCF-7 cells (400 μL, 6 × 10^4 cells) were incubated with 500 nM of hybridized aptamers in culture medium on ice for 40 min. After being washed twice, the cells were resuspended in culture medium and diluted 10-fold. Then, 100 μL of the cell suspension was introduced into the chip at different flow rates (10, 15, 20, and 25 μL·min^{-1}).

Followed by washing with PBS for 10 min (10 μL·min^{-1}); 100 μL of Hoechst 33342 (10 μg·mL^{-1}) was used to stain the captured cancer cells. The same amount of cell suspension was distributed on three wells of a 96-well plate to calculate the mean of cells flowed through the chip. Finally, we evaluated the specificity of the streptavidin-modified chip for the hybridized aptamer-tagged MCF-7 cells at a flow rate of 15 μL·min^{-1}. HEK-293T cells, WBCs, and MCF-7 cells without the hybridized aptamer were used as controls.

2.9 Cancer cell-release and viability assay

To evaluate the dissociation efficiency of biotinylated sequence A from hybridized aptamer-tagged cancer cells. MCF-7 cells (1 × 10^5) were first incubated with 500 nM of hybridized aptamers (sequence A was labeled with TAMRA), and then were resuspended in 100 μL of PBS containing 2 μM of sequence C_{30} or D_{30}. After incubation at 37 ˚C for 30 min, the cell suspension was centrifuged twice at 1,000 rpm for 8 min and resuspended in PBS for imaging. The fluorescence intensity of the cells before and after incubation with sequences C_{30} or D_{30} was calculated using Image J.

We then quantified the cancer cell-release efficiency. MCF-7 cells were prestained with Hoechst 33342 (10 μg·mL^{-1}) followed by incubation with hybridized aptamers. After capturing the cancer cells, 40 μL of sequence C_{30} and D_{30} (5 μM) were flowed through the chip, followed by incubation at 37 ˚C for 30 min, the chip was washed by PBS at a flow rate of 30 μL·min^{-1} for 5 min. Cells remaining on the chip were imaged and counted to calculate the release efficiency. To evaluate the viability of the retrieved cancer cells, released cancer cells were collected, stained with calcein-AM/PI, and further cultured. Live cells were stained by calcein-AM and dead cells were labeled by PI.

2.10 PCR analysis

To demonstrate that our method has the potential to detect protein biomarkers of retrieved cancer cells, sequence B on the surface of cancer cells was released using sequence D_{48} and amplified by PCR. Specifically, cells released from the chip (2000) in 100 μL of PBS were washed three times, and 0.5 μL of the supernatant was used as control for the PCR. Subsequently, a solution of sequence D_{48} (10 μL, 10 μM) was added to the released sequence B from cellular surface after incubation at 37 ˚C for 1.5 h. After centrifugation, 0.5 μL of the supernatant was used for PCR amplification.

PCR amplification was performed in a final volume of 25 μL, containing 12.5 μL of 2 × UltraSYBR Mixture, 2.5 μL of each of the primers (10 μM), 0.5 μL of supernatants of cell suspension or solutions with sequence B (0.1 nM), and 7 μL of PCR grade water. UltraSYBR Mixture was initially activated at 95 ˚C for 10 min, and then amplification was performed using the following thermal cycling conditions: 95 ˚C for 30 s, 52 ˚C for 30 s and 72 ˚C for 30 s. PCR products were analyzed using 12% gel electrophoresis.

2.11 Isolation and release of CTCs from cancer patient blood samples

Before isolation of CTCs from cancer patient blood samples, we first evaluated whether the hybridized aptamers could specifically recognize the target cancer cells. MCF-7 cells (6 × 10^3), prestained by Hoechst 33342, were spiked into lysed blood samples (1.0 mL of healthy human blood with red blood cells lysed) and incubated with 500 nM TAMRA-labeled hybridized aptamers in PBS for 40 min on ice. After washing twice, cells were resuspended in PBS for imaging.

Second, we quantified the cell-capture efficiency of mixture samples. A series of artificial blood samples were prepared by spiking prestained MCF-7 cells into lysed blood at densities of 26, 50, 175, and 550 cells per 0.5 mL. The same amount of cell suspension was distributed on three wells in a 96-well plate to calculate the mean of the cells spiked into the blood samples. Cell-capture experiments were performed using the optimized conditions described in section 2.8, and the captured MCF-7 cells were imaged and counted to calculate the recovery rate.

Finally, we isolated CTCs from breast cancer patient blood samples using the same conditions for capturing MCF-7 cells in the pure or mixed samples. One milliliter of whole blood samples in ethylenediaminetetraacetic acid (EDTA) blood collection tubes was treated by red blood cell lysis buffer following the standard protocol. The cell pellet was then resuspended in 400 μL

of PBS and incubated with 500 nM of hybridized aptamers on ice for 40 min. After washing, cells were resuspended in 200 μL of PBS and introduced to the chip at 15 μL·min^{-1} to capture the CTCs. Captured cells were fixed with 100 μL of 4% Perfluoroalkoxy alkane (PFA) (10 μL·min^{-1}), permeabilized with 100 μL of 0.2% triton X-100 (10 μL·min^{-1}), blocked with 5% BSA (30 min), and stained with 10 μg·mL^{-1} Hoechst 33342, FITC-labeled anti-CK19 monoclonal antibody and PE-labeled anti-CD45 monoclonal antibody (30 min). CTCs were identified as DAPI+/ CK+/ CD45- and WBCs were DAPI+/ CK-/ CD45+.

To characterize the retrieved CTCs, hybridized aptamer-tagged CTCs (sequence B was labeled TAMRA) were immunostained using the Alexa 488-conjugated anti-EpCAM antibody (0.2 μg·mL^{-1}) before incubation with sequence C_{30}. Thus, the surface of the retrieved CTCs showed strong red and green fluorescence.

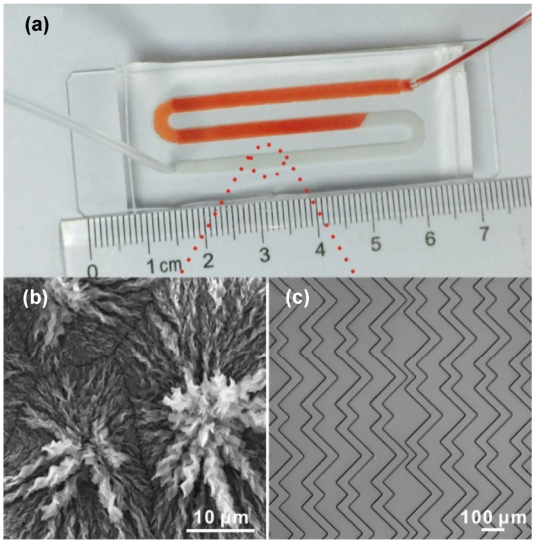

Figure 1 HZnPNS embedded microfluidic chip with herringbone microstructures. (a) Picture of HZnPNS integrated microchip with flowing blood. (b) SEM image of HZnPNS. (c) Micrograph of the grooved surface.

3 Results and discussion

3.1 Fabrication of the HZnPNS-embedded microchip

Many studies have shown that nanostructured substrates incorporated into microfluidic devices could address the problem of insufficient cell-capture efficiency through their high surface-area-to-volume ratio, increased capture agent presentation, and enhanced topographical interactions [14–18]. Furthermore, compared with regular-shaped nanosubstrates, such as vertically aligned nanopillars and horizontally packed nanofibers, substrates with hierarchical architectures provided more binding sites and better-matched topographical interactions [28–31]. In this work, we incorporated an overlaid PDMS chaotic mixer onto hierarchical substrates for high-performance CTC detection. As shown in Fig. 1, the as-prepared microchip comprises two components to enhance cell-substrate interaction. In the present study, our previously reported HZnPNS [31] were selected as the substrate of the chip given these factors: (1) HZnPNS are transparent, facilitating direct observation, imaging, and manipulation; (2) this substrate could be mildly etched by diluted HCl for patterning in combination with photolithography (Fig. S1 in the ESM); and (3) patterned hierarchical substrates could be easily bonded with the PDMS chamber after both were treated by plasma, without the help of chip holders. Figure 1(a) shows that blood could flow through the microchip uniformly without any leakage.

3.2 Design of DNA sequences for the capture and release of cancer cells

To endow DNA-responsive features on the HZnPNS-embedded microfluidic chip, we designed three single-stranded oligonucleotides (A, B, and C) that enable effective capture and release of the target cancer cells (Fig. S2 and Table S1 in the ESM). As shown in Fig. S2 in the ESM, sequence A was modified with biotin for immobilization on the streptavidin-coated surface of the chip. Sequence B contained three regions: A 20-nucleotide (nt) region that could hybridize with sequence A, a 48-nt region (aptamer) that could specifically recognize EpCAM-positive cancer cells [22, 27], and a 10-nt region that was used as a linker facilitating the accessibility of the aptamer to the target cancer cells, as well as a toehold for strand displacement. Note that the bases in the 20-nt and 10-nt regions of sequence B should not disturb the hairpin structure of the aptamer. Additionally, to make sure that aptamer-binding cells were firmly captured on the chip, hybridized aptamer (sequences A and B hybridized together, AB) should have a high melting

temperature (T_m). The T_m value of our designed hybridized aptamer was approximately 60 ℃ in PBS (OligoAnalyzer 3.1). Therefore, the hybridized aptamer is stable at room and physiological temperature. Increasing the number of base pairs commonly leads to more stable hybridization [41, 42], therefore, sequences C_{30}, with more bases (10 nt) than sequence A that were complementary to sequence B were used to induce dissociation of the hybridized aptamer, thereby releasing the captured cancer cells. Figure 2(a) shows that after incubation with sequence C_{30} at 37 ℃ for 30 min, the AB complex was almost completely dissociated via 10-nt toehold-mediated strand displacement (AB + C = A + BC). These data demonstrated that hybridization between the as-designed DNA sequences could be programmed under physiological conditions.

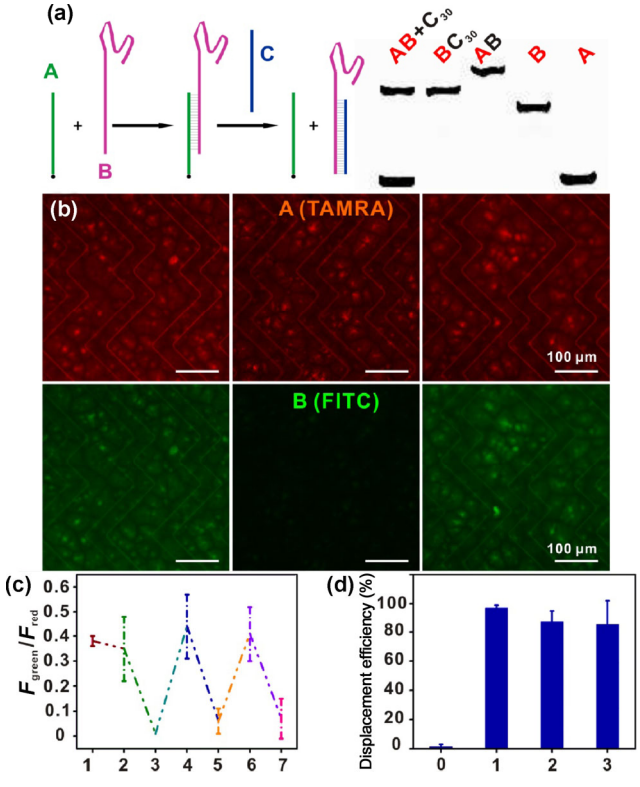

Figure 2 Nucleic acid hybridization. (a) 12% native polyacrylamide electrophoretic gel image of hybridization between sequences A, B, and C. Sequences A and B were labeled with TAMRA. (b) Fluorescent images of nucleic acid hybridization on a streptavidin-coated microchip. (c) Reversible fluorescence intensity of microchip modified with hybridized aptamers before and after incubation with sequence C_{30}. (d) Quantitative evaluation of the efficiency of strand displacement. Sequence A was modified with biotin and labeled by TAMRA. Sequence B was labeled by FITC. Error bars represent the standard deviation (n = 3).

3.3 Validation of the DNA-responsive microchip

After demonstrating the competitive hybridization between the above designed oligonucleotides, we assembled these oligonucleotides on the microchip. According to our previously reported method [31], plasma-treated chips were immediately incubated with the silane coupling agent containing carboxylate groups, and then activated to modify streptavidin (Fig. S3 in the ESM). Thus, via the streptavidin-biotin interaction, the hybridized aptamers were immobilized on the chip.

As shown in Figs. 2(b) and 2(c), hybridized aptamers on the chip are stable under physiological conditions. However, after treatment with sequence C_{30} at 37 ℃, the fluorescence intensity of the FITC-labeled sequence B dramatically decreased, while that of TAMRA-labeled sequence A showed no obvious change, suggesting that sequence C_{30} effectively induced the dissociation of sequence B from the hybridized aptamers, while sequence A remained tethered on the chip. When the chip was further incubated in a solution of sequence B, strong green fluorescence was recovered. Thus, sequence B could reversibly associate and dissociate with the sequence A-coated chip (Fig. 2(c)). Since ratiometric methods can avoid parameters such as optical path length and photobleaching, the ratio of green fluorescence to red fluorescence was used to quantify the strand displacement efficiency. Figure 2(d) displays the quantitative efficiency of strand displacement triggered by sequence C_{30} per cycle was more than 85%. These results indicated that we had successfully constructed a programmable DNA-responsive microchip by virtue of toehold-mediated strand displacement.

3.4 Cell-capture capability of the DNA-responsive microchip

Before performing the cell-capture experiment, we tested the specificity of anti-EpCAM aptamer for EpCAM-positive MCF-7 cells [14, 27]. Figure S4 in the ESM shows that the surface of the MCF-7 cells exhibited strong red fluorescence from the TAMRA-

labeled aptamer compared with EpCAM-negative HEK-293T cells [22] and white blood cells (WBCs). Considering that homogeneous method exhibited high cell-capture efficiency than heterogeneous method [43–45], target cancer cells were first recognized and tagged by the hybridized aptamers in the solution phase (homogeneous cell capture) before being introduced to the microchip (Fig. 3(a)). Figure S5 in the ESM shows that hybridized aptamers with biotin modification could bind to MCF-7 cells and further reacted with streptavidin, suggesting that streptavidin-coated microchips would enable the capture of hybridized aptamer-tagged target cancer cells via the high-affinity streptavidin-biotin interaction.

We then quantitatively assessed the effects of flow rate on cell-capture efficiency. The cell-capture efficiency was defined as the ratio of the number of target cells captured to the number of target cells initially introduced. The results in Fig. 3(b) show that the capture efficiency was approximately 90% for MCF-7 cells at flow rate 10 μL·min^{-1}, but decreased with increasing flow rates, primarily because of the reduced interaction time between the cells and substrates, as well as increased shear stress at higher flow rates. To obtain both efficient capture and sufficient throughput, 15 μL·min^{-1} (at which the capture efficiency was approximately 80%) was chosen as the optimum rate to enrich the target cancer cells.

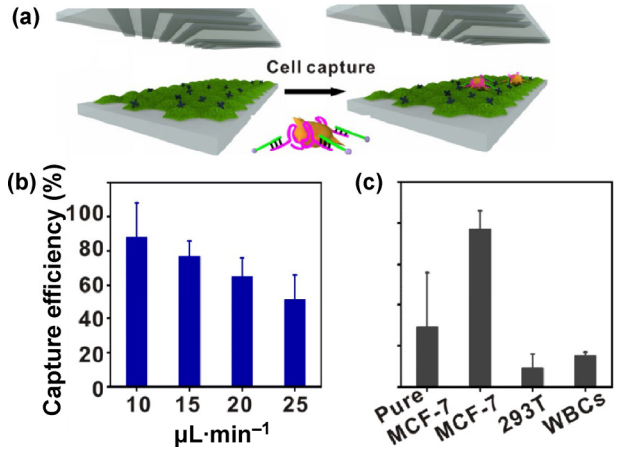

Figure 3 Cell-capture analysis. (a) Schematic representing the process of streptavidin-coated microchip for capturing hybridized aptamer-tagged target cancer cells. (b) Capture efficiency at flow rates from 10 to 25 μL·min^{-1}. (c) Specificity of the streptavidin-coated microchip for hybridized aptamer-tagged target cancer cells. Error bars represent the standard deviation (n = 3).

Meanwhile, we investigated the specificity of the streptavidin-modified microchip for the target cancer cells. As shown in Fig. 3(c), 77 ± 9% of hybridized aptamer-tagged MCF-7 cells were captured on the chip. However, EpCAM-negative cells (HEK-293T cells and WBCs) were captured with low efficiency (9 ± 7% and 15 ± 2%, respectively). For pure MCF-7 cells without hybridized aptamer conjugation, because of the enhanced topographical interaction between the surface structures of cancer cells and multiscale hierarchical architectures of HZnPNS, 29 ± 27% of cells nonspecifically bound to the chip, which was consistent with our previous results [31]. These data clearly showed that the target cancer cells could be specifically and efficiently captured on the microchip, benefitting from homogeneous recognition, improved topographical interactions, and the high-affinity streptavidin-biotin interaction.

3.5 Cell release and viability assay

We evaluated the cell-release performance via toehold-mediated strand displacement. Sequence C_{30} could compete against sequence A to hybridize and release sequence B with the help of a 10-nt toehold sequence, resulting in dramatically weakened cell-surface interaction. Before cell release, we investigated the strand displacement reaction on the cell surface. As indicated in Figs. 4(b) and 4(c), after incubation with sequence C_{30} at 37 ˚C for 30 min, the fluorescence intensity of cell surface was significantly diminished (by more than 90%), because of the dissociation of sequence A from the cells. However, hybridization of sequence D_{30} with the cell-bound anti-EpCAM aptamers (Fig. 4(a)) caused a 74% reduction in fluorescence under the same conditions. The difference between these two results could possibly be attributed to the fact that sequence C_{30} hybridizes easily via the toehold region with the non-aptamer region of sequence B, while sequence D_{30} competitively hybridizes with the cell-bound aptamer region via a unique hairpin structure. Next, we quantitatively assessed the cell-release efficiency (as a percentage of captured cells). Compared with the lower cell-release efficiency (43 ± 14%) induced by sequence D_{30}, sequences C_{30} caused 86 ± 1% of cancer cells released from the chip (Fig. 4(d)).

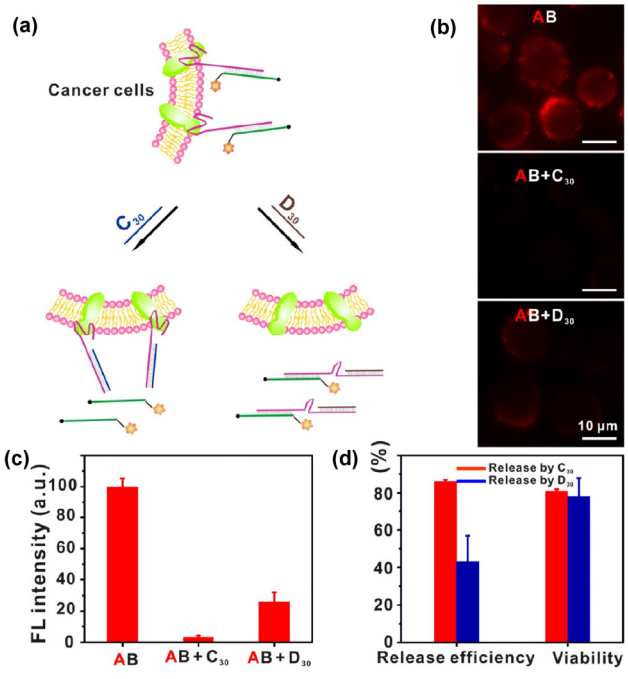

Figure 4 Cell-release assay. (a) Schematic representing two ways to release target cancer cells from microchip by sequences C_{30} and D_{30}. Fluorescent images (b) and normalized fluorescence intensity (c) of hybridized aptamer-tagged MCF-7 cells before and after incubation with sequence C_{30} and D_{30}. Sequences A were labeled by TAMRA. (d) Quantitative evaluation of the release efficiency and viability of retrieved cancer cells. Error bars represent the standard deviation (n = 3).

To evaluate the viability of the retrieved cancer cells, calcein-AM and propidium iodide (PI) were used to stain live and dead cells, respectively (Fig. S6(a) in the ESM). The majority of released cells exhibited good viability (81 ± 1%) and no significant difference was observed in the viability of the retrieved cancer cells between sequence C_{30} and D_{30}-triggered cell release (Fig. 4(d)). Furthermore, the retrieved cancer cells spread well after cultivation for 24 h (Fig. S6(b) in the ESM). Taken together, the DNA-responsive microchip enables effective and gentle release of captured target cancer cells via strand displacement.

3.6 PCR analysis of retrieved cancer cells

To demonstrate that our method enabled further characterization and detection of retrieved cancer cells, aptamer-containing sequence B bound on the surface EpCAM of the retrieved cancer cells was amplified by PCR. As shown in Figs. 5(a) and 5(b), the red fluorescence signal was still detected from the surface of the cancer cells released from the chip, indicating that sequence B remains on the retrieved cell surface. To facilitate PCR analysis, sequence D_{48}, which is complementary to the anti-EpCAM aptamer, was used to fast release sequence B from the cell surface (Fig. S7 in the ESM) [23]. Figure 5(c) shows that our designed primers could specifically amplify sequence B (2 pM) without interference from other oligonucleotides (A, C, and D). Figure 5(d) shows that sequence B in the supernatant of retrieved cancer cells after incubation with sequences D_{48} showed a significant band on the gel, compared with the control sample (without sequence D_{48} treatment). The detectable signal from the control sample using sensitive qRT-PCR was possibly attributed to the dissociation of sequences B from cellular surface after long-term sample handling (the dissociation constant (K_d) of the anti-EpCAM aptamer was approximately 38 nM) [22]. These results indicated that the EpCAM signatures of the cancer cells released by strand displacement could be transformed into a detectable signal via PCR amplification, providing evidence for the potential analysis of protein biomarkers and for characterization

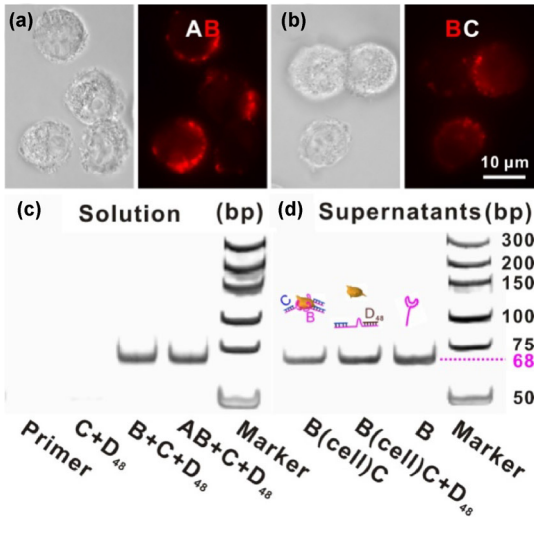

Figure 5 Analysis of retrieved cancer cells by qRT-PCR. Fluorescent images of cancer cells before (a) and (b) after release from the chip. Sequence B was labeled by TAMRA. (c) Gel analysis of PCR products of solution with or without 2 pM of sequence B. (d) Analysis of sequence B in supernatants of retrieved from cancer cells before and after incubation with sequence D_{48} against cellular surface epithelial cell adhesion molecule (EpCAM). Sequence B was amplified and detected after 40 cycles of PCR. (ΔC_t value was 2.31).

of CTCs. Taken together, the as-prepared microchip not only enables the capture, release, and detection of EpCAM biomarkers of cancer cells, but could also be readily customized to detect other molecules or biomarkers using their corresponding aptamers.

3.7 Isolation and release of CTCs from cancer patients′ blood samples

To further evaluate its clinical performance, the DNA-responsive microchip was applied to detect CTCs from cancer patients' blood samples. In a preliminary experiment, we evaluated the cell-capture performance of MCF-7 cells spiked into lysed blood samples. As shown in Fig. S8(a) in the ESM, target cancer cells spiked into healthy blood samples from which the red blood cells had been removed, could be specifically and effectively recognized by the hybridized aptamers. Moreover, a good linear correlation between of the number of spiked and captured cells (R^2 = 0.99996, n = 3) was observed in Fig. S8(b) in the ESM, and 64% of the MCF-7 cells were detected from the lysed blood samples. The patients' blood samples with lysed red blood cells were introduced into the microchip for CTC capture, followed by immunostaining to identify CTCs and WBCs. We scored as CTCs those that were DAPI+/CK+/CD45− (30 μm > cell sizes > 10 μm), and as WBCs those that were DAPI+/CK−/CD45+ (cell sizes < 15 μm) (Fig. 6(a)). The CTC-capture results from 10 blood samples are summarized in Fig. 6(b). Additionally, we released captured CTCs utilizing above optimized release conditions. Captured CTCs were bound with Alexa 488-conjugated anti-EpCAM antibody before release to further demonstrate that the CTCs were successfully released from the microchip. As shown in Fig. 6(c), red fluorescence of the aptamer and green fluorescence of the antibody colocalized on the surface of retrieved CTCs, because the binding site of anti-EpCAM aptamer on EpCAM is different from that of the anti-EpCAM antibody [22]. These results demonstrated the clinical potential of the as-prepared microchip to detect CTCs.

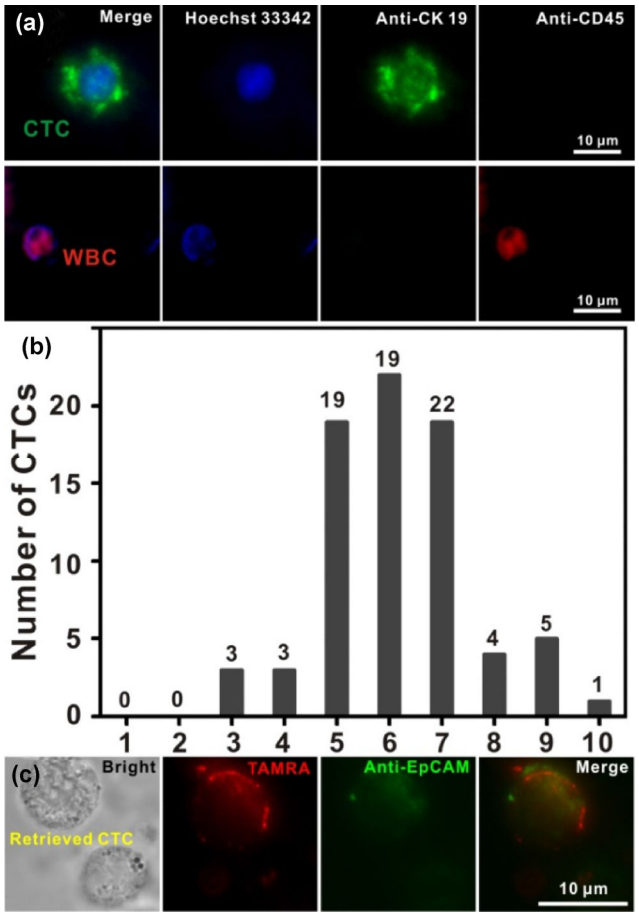

Figure 6 Circulating tumor cells (CTCs) detection. (a) Fluorescent images of CTCs isolated from a breast cancer patient's blood sample. (b) Quantitative results of CTCs enumerated from 10 blood samples including cancer patient blood samples (3–10) and healthy human blood samples (1–2). (c) Fluorescent images of retrieved CTCs. Sequences B of hybridized aptamers was labeled by carboxytetramethylrhodamine (TAMRA) and anti-epithelial cell adhesion molecule (EpCAM) antibody was conjugated with Alexa 488.

4 Conclusions

In summary, we successfully developed a programmable DNA-responsive microchip for the capture, release, and detection of CTCs. In addition to the herringbone structure for enhanced cell-surface interaction, the as-prepared microchip was also well integrated with hierarchical substrates, producing more binding sites and better-matched topographical interaction for high-performance cell capture. Toehold-mediated strand displacement, which does not involve potentially destructive factors for cells or substrates, gently and effectively released the captured cancer cells from the microchip. More importantly, the surface protein signatures of the cancer cells retrieved using our approach could be transformed into a detectable signal via PCR amplification, thus providing a

promising way toward quantitative analysis of CTC biomarkers. While having demonstrated the capability of this microchip to capture and release CTCs in patients′ blood samples, we ultimately anticipate that more and detailed information could be extracted from CTCs. This will advance our understanding of the mechanisms underlying tumor metastasis.

Acknowledgements

This work was supported by the National Natural Science Foundation of China (NSFC) (Nos. 21432008, 91413109 and 21575110). China Postdoctoral Innovative Talent Support Program of China (No. BX201700176).

Electronic Supplementary Material: Supplementary material (the patterning process of hierarchical substrates (Fig. S1), detailed nucleic acid hybridization (Fig. S2), microscopic images (Figs. S3–S8), DNA sequences (Table S1) and quantitative CTC detection from patients′ blood (Table S2)) is available in the online version of this article at https://doi.org/10.1007/s12274-017-1885-8.

References

[1] Alix-Panabières, C.; Pantel, K. Challenges in circulating tumour cell research. *Nat. Rev. Cancer* **2014**, *14*, 623–631.

[2] Paterlini-Brechot, P.; Benali, N. L. Circulating tumor cells (CTC) detection: Clinical impact and future directions. *Cancer Lett.* **2007**, *253*, 180–204.

[3] Park, J. M.; Lee, J. Y.; Lee, J. G.; Jeong, H.; Oh, J. M.; Kim, Y. J.; Park, D.; Kim, M. S.; Lee, H. J.; Oh, J. H. et al. Highly efficient assay of circulating tumor cells by selective sedimentation with a density gradient medium and microfiltration from whole blood. *Anal. Chem.* **2012**, *84*, 7400–7407.

[4] Seal, S. H. A sieve for the isolation of cancer cells and other large cells from the blood. *Cancer* **1964**, *17*, 637–642.

[5] Lee, H. J.; Oh, J. H.; Oh, J. M.; Park, J. M.; Lee, J. G.; Kim, M. S.; Kim, Y. J.; Kang, H. J.; Jeong, J.; Kim, S. I. et al. Efficient isolation and accurate *in situ* analysis of circulating tumor cells using detachable beads and a high-pore-density filter. *Angew. Chem., Int. Ed.* **2013**, 52, 8337–8340.

[6] Tang, Y. D.; Shi, J.; Li, S. S.; Wang, L.; Cayre, Y. E.; Chen, Y. Microfluidic device with integrated microfilter of conical-shaped holes for high efficiency and high purity capture of circulating tumor cells. *Sci. Rep.* **2014**, *4*, 6052.

[7] Cristofanilli, M.; Budd, G. T. ; Ellis, M. J.; Stopeck, A.; Matera, J.; Miller, M. C.; Reuben, J. M.; Doyle, G. V.; Allard, W. J.; Terstappen, L. W. et al. Circulating tumor cells, disease progression, and survival in metastatic breast cancer. *N. Engl. J. Med.* **2004**, *351*, 781–791.

[8] Wen, C. Y.; Wu, L. L.; Zhang, Z. L.; Liu, Y. L.; Wei, S. Z.; Hu, J.; Tang, M.; Sun, E. Z.; Gong, Y. P.; Yu, J. et al. Quick-response magnetic nanospheres for rapid, efficient capture and sensitive detection of circulating tumor cells. *ACS Nano* **2014**, *8*, 941–949.

[9] Xie, M.; Lu, N. N.; Cheng, S. B.; Wang, X. Y.; Wang, M.; Guo, S.; Wen, C. Y.; Hu, J.; Pang, D. W.; Huang, W. H. Engineered decomposable multifunctional nanobioprobes for capture and release of rare cancer cells. *Anal. Chem.* **2014**, *86*, 4618–4626.

[10] Wang, S. T.; Wang, H.; Jiao, J.; Chen, K. J.; Owens, G. E.; Kamei, K.; Sun, J.; Sherman, D. J.; Behrenbruch, C. P.; Wu, H. et al. Three-dimensional nanostructured substrates toward efficient capture of circulating tumor cells. *Angew. Chem., Int. Ed.* **2009**, *48*, 8970–8973.

[11] Zhang, N. G.; Deng, Y. L.; Tai, Q. D.; Cheng, B. R.; Zhao, L. B.; Shen, Q. L.; He, R. X.; Hong, L. Y.; Liu, W.; Guo, S. S. et al. Electrospun TiO_2 nanofiber-based cell capture assay for detecting circulating tumor cells from colorectal and gastric cancer patients. *Adv. Mater.* **2012**, *24*, 2756–2760.

[12] Nagrath, S.; Sequist, L. V.; Maheswaran, S.; Bell, D. W.; Irimia, D.; Ulkus, L.; Smith, M. R.; Kwak, E. L.; Digumarthy, S.; Muzikansky, A. et al. Isolation of rare circulating tumour cells in cancer patients by microchip technology. *Nature* **2007**, *450*, 1235–1239.

[13] Stott, S. L.; Hsu, C. H.; Tsukrov, D. I.; Yu, M.; Miyamoto, D. T.; Waltman, B. A.; Rothenberg, S. M.; Shah, A. M.; Smas, M. E.; Korir, G. K. et al. Isolation of Circulating tumor cells using a microvortex-generating herringbone-chip. *Proc. Natl. Acad. Sci. USA* **2010**, *107*, 18392–18397.

[14] Wang, S. T.; Liu, K.; Liu, J.; Yu, Z. T. F.; Xu, X. W.; Zhao, L. B.; Lee, T.; Lee, E. K.; Reiss, J.; Lee, Y. K. et al. Highly efficient capture of circulating tumor cells by using nanostructured silicon substrates with integrated chaotic micromixers. *Angew. Chem., Int. Ed.* **2011**, *50*, 3084–3088.

[15] Yoon, H. J.; Kim, T. H.; Zhang, Z.; Azizi, E.; Pham, T. M.; Paoletti, C.; Lin, J.; Ramnath, N.; Wicha, M. S.; Hayes, D. F. et al. Sensitive capture of circulating tumour cells by functionalized graphene oxide nanosheets. *Nat. Nanotechnol.* **2013**, *8*, 735–741.

[16] Shen, Q. L.; Xu, L.; Zhao, L. B.; Wu, D. X.; Fan, Y. S.; Zhou, Y. L.; Ouyang, W. H.; Xu, X. C.; Zhang, Z.; Song, M. et al. Specific capture and release of circulating tumor cells

using aptamer-modified nanosubstrates. *Adv. Mater.* **2013**, *25*, 2368–2373.

[17] Sheng, W. A.; Chen, T.; Tan, W. H.; Fan, Z. H. Multivalent DNA nanospheres for enhanced capture of cancer cells in microfluidic devices. *ACS Nano* **2013**, *7*, 7067–7076.

[18] Park, M. H.; Reátegui, E.; Li, W.; Tessier, S. N.; Wong, K. H. K.; Jensen, A. E.; Thapar, V.; Ting, D.; Toner, M.; Stott, S. L. et al. Enhanced isolation and release of circulating tumor cells using nanoparticle binding and ligand exchange in a microfluidic chip. *J. Am. Chem. Soc.* **2017**, *139*, 2741–2749.

[19] Cheng, S. B.; Xie, M.; Xu, J. Q.; Wang, J.; Lv, S. W.; Guo, S.; Shu, Y.; Wang, M.; Dong, W. G.; Huang. W. H. High-efficiency capture of individual and cluster of circulating tumor cells by a microchip embedded with three-dimensional poly(dimethylsiloxane) scaffold. *Anal. Chem.* **2016**, *88*, 6773–6780.

[20] Adams, A. A.; Okagbare, P. I.; Feng, J.; Hupert, M. L.; Patterson, D.; Göttert, J.; McCarley, R. L.; Nikitopoulos, D.; Murphy, M. C.; Soper, S. A. Highly efficient circulating tumor cell isolation from whole blood and label-free enumeration using polymer-based microfluidics with an integrated conductivity sensor. *J. Am. Chem. Soc.* **2008**, *130*, 8633–8641.

[21] Labib, M.; Green, B.; Mohamadi, R. M.; Mepham, A.; Ahmed, S. U.; Mahmoudian, L.; Chang, I. H.; Sargent, E. H.; Kelley S. O. Aptamer and antisense-mediated two-dimensional isolation of specific cancer cell subpopulations. *J. Am. Chem. Soc.* **2016**, *138*, 2476–2479.

[22] Song, Y. L.; Zhu, Z.; An, Y.; Zhang, W. T.; Zhang, H. M.; Liu, D.; Yu, C. D.; Duan, W.; Yang, C. J. Selection of DNA aptamers against epithelial cell adhesion molecule for cancer cell imaging and circulating tumor cell capture. *Anal. Chem.* **2013**, *85*, 4141–4149.

[23] Wan, Y.; Liu, Y. L.; Allen, P. B.; Asghar, W.; Mahmood, M. A. I.; Tan, J. F.; Duhon, H.; Kim,Y. T.; Ellingtone A. D.; Iqbal, S. M. Capture, isolation and release of cancer cells with aptamer-functionalized glass bead array. *Lab Chip* **2012**, *12*, 4693–4701.

[24] Fang, S.; Wang, C.; Xiang, J.; Cheng, L.; Song, X. J.; Xu, L. G.; Peng, R.; Liu, Z. Aptamer-conjugated upconversion nanoprobes assisted by magnetic separation for effective isolation and sensitive detection of circulating tumor cells. *Nano Res.* **2014**, *7*, 1327–1336.

[25] Qiu, J. C.; Zhao, K.; Li, L. L.; Yu, X.; Guo, W. B.; Wang, S.; Zhang, X. D.; Pan, C. F.; Wang, Z. L.; Liu, H. A titanium dioxide nanorod array as a high-affinity nano-bio interface of a microfluidic device for efficient capture of circulating tumor cells. *Nano Res.* **2017**, *10*, 776–784.

[26] Wu, L.; Ji, H. W.; Guan, Y. J.; Ran, X.; Ren, J. S.; Qu, X. G. A graphene-based chemical nose/tongue approach for the identification of normal, cancerous and circulating tumor cells. *NPG Asia Mater.* **2017**, *9*, e356.

[27] Wang, Z. L.; Sun, N.; Liu, M.; Cao, Y.; Wang, K. W.; Wang, J. E.; Pei, R. J. Multifunctional nanofibers for specific purification and release of CTCs. *ACS Sens.* **2017**, *2*, 547–552.

[28] Zhang, P. C.; Chen, L.; Xu, T. L.; Liu, H. L.; Liu, X. L.; Meng, J. X.; Yang, G.; Jiang, L.; Wang, S. T. Programmable fractal nanostructured interfaces for specific recognition and electrochemical release of cancer cells. *Adv. Mater.* **2013**, *25*, 3566–3570.

[29] Zhang, F. L.; Jiang, Y.; Liu, X. L.; Meng, J. X.; Zhang, P. C.; Liu, H. L.; Yang, G.; Li, G. N.; Jiang, L.; Wan, L. J. et al. Hierarchical nanowire arrays as three-dimensional fractal nanobiointerfaces for high efficient capture of cancer cells. *Nano Lett.* **2016**, *16*, 766–772.

[30] Meng, J. X.; Zhang, P. C.; Zhang, F. L.; Liu, H. L.; Fan, J. B.; Liu, X. L.; Yang, G.; Jiang, L.; Wang, S. T. A Self-cleaning TiO_2 nanosisal-like coating toward disposing nanobiochips of cancer detection. *ACS Nano* **2015**, *9*, 9284–9291.

[31] Guo, S.; Xu, J. Q.; Xie, M.; Huang, W.; Yuan, E. F.; Liu, Y.; Fan, L. P.; Cheng, S. B.; Liu, S. M.; Wang, F. B. et al. Degradable zinc-phosphate-based hierarchical nanosubstrates for capture and release of circulating tumor cells. *ACS Appl. Mater. Interfaces* **2016**, *8*, 15917–15925.

[32] Zhang, L. Q.; Wan, S.; Jiang, Y.; Wang, Y. Y.; Fu, T.; Liu, Q. L.; Cao, Z. J.; Qiu, L. P.; Tan, W. H. Molecular elucidation of disease biomarkers at the interface of chemistry and biology. *J. Am. Chem. Soc.* **2017**, 139, 2532–2540.

[33] Lv, S. W.; Wang, J.; Xie, M.; Lu, N. N.; Li, Z.; Yan, X. W.; Cai, S. L.; Zhang, P. A.; Dong, W. G.; Huang, W. H. Photoresponsive immunomagnetic nanocarrier for capture and release of rare circulating tumor cells. *Chem. Sci.* **2015**, *6*, 6432–6438.

[34] Li, W.; Wang, J. S.; Ren, J. S.; Qu, X. G. Near-infrared upconversion controls photocaged cell adhesion. *J. Am. Chem. Soc.* **2014**, *136*, 2248–2251.

[35] Jeon, S.; Moon, J. M.; Lee, E. S.; Kim, Y. H.; Cho, Y. An electroactive biotin-doped polypyrrole substrate that immobilizes and releases EpCAM-positive cancer cells. *Angew. Chem., Int. Ed.* **2014**, *53*, 4597–4602.

[36] Reátegui, E.; Aceto, N.; Lim, E. J.; Sullivan, J. P.; Jensen, A. E.; Zeinali, M.; Martel, J. M.; Aranyosi, A. J.; Li, W.; Castleberry, S. et al. Tunable nanostructured coating for the capture and selective release of viable circulating tumor cells. *Adv. Mater.* **2015**, *27*, 1593–1599.

[37] Hou, S.; Zhao, H. C.; Zhao, L. B.; Shen, Q. L.; Wei, K. S.; Suh, D. Y.; Nakao, A.; Garcia, M. A.; Song, M.; Lee, T. et al.

Capture and stimulated release of circulating tumor cells on polymer-grafted silicon nanostructures. *Adv. Mater.* **2013**, *25*, 1547–1551.

[38] Lv, S. W.; Liu, Y.; Xie, M.; Wang, J.; Yan, X. W.; Li, Z.; Dong, W. G.; Huang, W. H. Near-infrared light-responsive hydrogel for specific recognition and photothermal site-release of circulating tumor cells. *ACS Nano* **2016**, *10*, 6201–6210.

[39] Huang, Q. Q.; Chen, B. L.; He, R. X.; He, Z. B.; Cai, B.; Xu, J. H.; Qian, W. Y.; Chan, H. L.; Liu, W.; Guo, S. S. et al. Capture and release of cancer cells based on sacrificeable transparent MnO_2 nanospheres thin film. *Adv. Healthcare Mater.* **2014**, *3*, 1420–1425.

[40] Liu, H. L.; Li, Y. Y.; Sun, K.; Fan, J. B.; Zhang, P. C.; Meng, J. X.; Wang, S. T.; Jiang, L. Dual-responsive surfaces modified with phenylboronic acid-containing polymer brush to reversibly capture and release cancer cells. *J. Am. Chem. Soc.* **2013**, *135*, 7603–7609.

[41] Zhang, Z. Y.; Chen, N. C.; Li, S. H.; Battig, M. R.; Wang, Y. Programmable hydrogels for controlled cell catch and release using hybridized aptamers and complementary sequences. *J. Am. Chem. Soc.* **2012**, *134*, 15716–15719.

[42] Delport, F.; Pollet, J.; Janssen, K.; Verbruggen, B.; Knez, K.; Spasic, D.; Lammertyn, J. Real-time monitoring of DNA hybridization and melting processes using a fiber optic sensor. *Nanotechnology* **2012**, *23*, 065503.

[43] Kwong, G. A.; Radu, C. G.; Hwang, K.; Shu, C. J.; Ma, C.; Koya, R. C.; Comin-Anduix, B.; Hadrup, S. R.; Bailey, R. C.; Witte, O. N. et al. Modular nucleic acid assembled p/MHC microarrays for multiplexed sorting of antigen-specific T cells. *J. Am. Chem. Soc.* **2009**, *131*, 9695–9703.

[44] Vermesh, U.; Vermesh, O.; Wang, J.; Kwong, G. A.; Ma, C.; Hwang, K.; Heath, J. R. High-density, multiplexed patterning of cells at single-cell resolution for tissue engineering and other applications. *Angew. Chem., Int. Ed.* **2011**, *50*, 7378–7380.

[45] Deng, Y. L.; Zhang, Y.; Sun, S.; Wang, Z. H.; Wang, M. J.; Yu, B. Q.; Czajkowsky, D. M.; Liu, B. Y.; Li, Y.; Wei, W. et al. An integrated microfluidic chip system for single-cell secretion profiling of rare circulating tumor cells. *Sci. Rep.* **2014**, *4*, 7499.